Numerical Study of an Additive Schwarz Preconditioner for a Thin Membrane Diffusion Problem

Piotr Krzyżanowski

1 Introduction

In the biology of the cell one has to take into account the situation when two different materials — for example, the cytoplasm and the nucleus — are separated by a permeable membrane. Chemicals inside the cell diffuse not only inside both the nucleus and in the cytoplasm, but they also pass through the membrane as well. A mathematical model of such phenomenon, which gained some popularity (see e.g. [7, 14] and the literature therein) has been introduced by Kedem and Kachalsky, where a system of diffusive PDEs is coupled by specific boundary conditions on the inner interface. In this paper we will investigate a simplified problem, hoping our approach may be applicable to more complicated cases as well.

Let us denote by $\Omega \subset R^d$ ($d = 2, 3$) the domain occupied by the cell. It naturally decomposes into disjoint open sets: the surrounding cytoplasm Ω_1 and $N - 1$ organelles (the nucleus, mitochondria, etc.), denoted here $\Omega_2, \ldots, \Omega_N$, so that $\bar{\Omega} = \bigcup_{i=1}^{N} \bar{\Omega}_i$ and $\Omega_i \cap \Omega_j = \emptyset$, cf. Figure 1. The interface between the i-th organelle and the outer cell will be denoted $\Gamma_i = \partial\Omega_1 \cap \partial\Omega_i = \partial\Omega_i$ and for the simplicity of the notation we set $\Gamma = \bigcup_{i=2}^{N} \bar{\Gamma}_i$. Our model problem reads:

$$-\operatorname{div}(\varrho_i \nabla u_i) + K_i u_i = F_i \text{ in } \Omega_i, \qquad i = 1, \ldots, N, \tag{1}$$

with interface conditions

$$-\varrho_1 \nabla u_1 \cdot n_1 = G_i \cdot (u_1 - u_i) = \varrho_i \nabla u_i \cdot n_i \text{ on } \Gamma_i \tag{2}$$

for $i = 2, \ldots, N$, where n_i denotes the unit outer normal vector to Ω_i. The system is completed with a non-permeability external boundary condition,

Piotr Krzyżanowski

Faculty of Mathematics, Informatics and Mechanics, University of Warsaw, Poland, e-mail: `p.krzyzanowski@mimuw.edu.pl`

$$-\varrho_1 \nabla u_1 \cdot n = 0 \text{ on } \partial\Omega. \tag{3}$$

Here, $\varrho_1, \ldots, \varrho_N$ and $K_1, \ldots, K_N$ are prescribed positive constants, which can be different between the subdomains. For the source terms we assume $F_i \in L^2(\Omega_i)$, $i = 1, \ldots, N$. The unknown functions u_i defined in $\bar{\Omega}_i$, $i = 1, \ldots, N$ may represent e.g. the hes1 mRNA concentration in the cell [14].

Positive constant parameters G_i model the thickness of the interface; roughly speaking, the permeability constant $G_i \sim 1/H_i$, where H_i is the thickness of the membrane between Ω_i and Ω_1; therefore for thin interfaces $G_i \gg 1$. In order to address the interface conditions (2), we incorporate them directly into the bilinear form, obtaining the following weak formulation of (1)–(3):

Problem 1 Find $(u_1, \ldots, u_N) \in V = H^1(\Omega_1) \times \cdots \times H^1(\Omega_N)$ such that

$$\sum_{i=1}^{N} \int_{\Omega_i} \varrho_i \nabla u_i \cdot \nabla \varphi_i + K_i u_i \varphi_i \, dx + \sum_{i=2}^{N} \int_{\Gamma_i} G_i (u_i - u_1)(\varphi_i - \varphi_1) \, ds = \sum_{i=1}^{N} \int_{\Omega_i} F_i \varphi_i \, dx$$

for all $(\varphi_1, \ldots, \varphi_N) \in V$.

The bilinear form appearing in Problem 1 is symmetric and elliptic. Note that the interface integral term in Problem 1 results from the permeability condition (2) and it penalizes the jump of the solution across the interface Γ.

We discretize Problem 1 with a composite discontinuous Galerkin h-p finite element method [8]. Inside Ω_i, we use a continuous h-p method, while allowing for the discontinuity of the solution across Γ. In order not to complicate the exposition, we will assume from now on that each Ω_i is a polyhedron.

Let us define a simplicial, quasi-uniform, conforming triangulation $\mathcal{T}_h$ with mesh size h over Ω, whose elements are aligned with Ω_i, so that Γ crosses no element in $\mathcal{T}_h$. In this way each Ω_i, $i = 1, \ldots, N$ is supplied with its own triangulation $\mathcal{T}_h(\Omega_i)$. We define the corresponding local continuous finite element spaces as

$$V_h^p(\Omega_i) = \{v \in C(\Omega_i) : v_{|K} \in \mathcal{P}^p(K) \quad \forall K \in \mathcal{T}_h(\Omega_i)\},$$

where $\mathcal{P}^p$ is the space of polynomials of degree at most $p \geq 1$. The finite element approximation of Problem 1 then reads:

Problem 2 Find $u \in V_h^p = \{v \in L^2(\Omega) : v_{|\Omega_i} \in V_h^p(\Omega_i), \quad i = 1, \ldots, N\}$ such that $\mathcal{A}(u, v) = \sum_{i=1}^{N} \int_{\Omega_i} F_i \varphi_i \, dx$ for all $\varphi \in V_h^p$, where

$$\mathcal{A}(u, v) = \sum_{i=1}^{N} \int_{\Omega_i} \varrho_i \nabla u_i \cdot \nabla \varphi_i + K_i u_i \varphi_i \, dx + \sum_{i=2}^{N} \int_{\Gamma_i} G_i \cdot (u_i - u_1)(\varphi_i - \varphi_1) \, ds$$

Our goal in this paper is to describe and experimentally evaluate the performance of a preconditioner for Problem 2, based on the additive Schwarz method, see e.g. [15], in terms of the convergence rate of the preconditioned conjugate gradients iterative solver. The penalty constant G_i is an independent parameter of the original

problem, in contrast to the analogous term in the interior penalty discontinuous Galerkin method. For the latter, a preconditioner for Poisson equation with $\varrho_i = 1$ was developed and proved optimal with respect to discretization and penalty constant in [5], where numerical evidence was provided that this method leads to the condition number which grows linearly with the contrast ratio in the diffusion coefficient. Another approach was considered in [9] and [12], where it was proved the convergence rate is uniformly bounded with respect to diffusion coefficient jumps; however, the dependence on the penalizing constant was not investigated. Here, we provide extensive tests of the preconditioning properties of a method first introduced in [13], which is inspired by [5] and [12]. It turns out that the method considered here is robust with respect to both the problem's parameters and to discretization parameters as well.

The rest of paper is organized as follows. In Section 2, a preconditioner based on the additive Schwarz method for solving Problem 2 is presented. We report on its performance in a series of numerical experiments in Section 3. We conclude with final remarks in Section 4.

2 Additive Schwarz preconditioner

In this section we consider a preconditioner based on the nonoverlapping additive Schwarz method, first proposed, in a different setting, in [2] and later developed in many papers, including [9, 4, 12, 3]. The space V_h^p is decomposed as follows:

$$V_h^p = V_0 + \sum_{i=1}^{N} V_i,$$

where for $i = 1, \ldots, N$ the local spaces are

$$V_i = \{v \in V_h^p : v_{|\Omega_j} = 0 \text{ for all } j \neq i\},$$

so that V_i is a zero–extension of functions from $V_h^p(\Omega_i)$. Note that V_h^p is already a direct sum of these local spaces. In the setting of Problem 2, the main goal of the coarse space V_0 is to deal with the penalization term; we define V_0 as the finite element space of piecewise polynomial functions which are continuous in entire Ω,

$$V_0 = \{v \in C(\Omega) : v_{|K} \in \mathcal{P}^p(K) \text{ for all } K \in \mathcal{T}_h\}.$$

The choice of the coarse space is inspired by the work by Antonietti et al. [5] for the standard Poisson problem and notably leads to a problem whose number of unknowns is smaller than the original only by a small fraction.

As mentioned above, $\mathcal{A}(\cdot, \cdot)$ is symmetric positive definite on $V_h^p \subset V$. We define operators $T_i : V_h^p \to V_i$, $i = 0, 1, \ldots, N$, by "inexact" solvers $A_i(T_i u, v) = \mathcal{A}(u, v) \, \forall v \in V_i$. We will assume that $A_i(\cdot, \cdot)$ are symmetric, positive definite, and

they induce a linear operator which is spectrally equivalent to the operator induced by $\mathcal{A}(\cdot, \cdot)$ on V_i. The preconditioned operator is

$$T = T_0 + \sum_{i=1}^{N} T_i. \tag{4}$$

While all T_i, $i = 0, 1, \ldots, N$, can be applied in parallel, the performance of the preconditioner is affected by the specific choice of subspace solvers $A_i(\cdot, \cdot)$. In the experiments in the following section, we will choose the algebraic multigrid (AMG) solvers, see e.g. [16]. In particular, it is well known that AMG can be a robust preconditioner for discontinuous coefficient problems discretized with continuous finite elements, so a parallel AMG makes a reasonable choice for the inexact solver on V_0 (other choices, e.g. the additive average Schwarz method [10], are also possible).

From the definition of T_i it follows that virtually all degrees of freedom are solved twice when T is applied, so there is room for the improvement of the complexity of the method. On the other hand, as it will be shown in the following section, the method converges independently of the size of the permeability coefficients.

3 Numerical experiments

Since the number of problem parameters is large we restrict ourselves to the case when $\varrho_1 = K_1 = 1$ and $\varrho_2 = \ldots = \varrho_N$, $K_2 = \ldots = K_N$ and $G_2 = \ldots = G_N = G$. Our goal in this section is to investigate the influence of various parameters of the problem: the diffusion coefficient contrast $\varrho = \varrho_2/\varrho_1$, the reaction coefficient contrast $K = K_2/K_1$, the value of the permeability coefficient G, the number of subdomains N, and discretization parameters: the mesh size and the polynomial degree, on the convergence rate of the preconditioned conjugate gradients (PCG) iteration and the condition number of T. Our implementation is based on the FEniCS software [1] with PETSc [6] as the linear algebra backend. For the inexact solvers on the subspaces we chose the algebraic multigrid method: BoomerAMG solver from the hypre library [11], with default parameters. We performed tests for Ω in 2D and 3D; example domains are depicted in Figure 1. The organelles were allowed to touch neither the boundary of the domain, nor other organelles.

The domain Ω was triangulated with unstructured, quasi-uniform mesh with resolution parameter r, roughly proportional to h^{-1}. For the finite element polynomial degrees $1 \leq p \leq 3$ this resulted in discrete problem sizes summarized in Table 1.

In tables below, we report the number of iterations required to reduce the initial residual norm by a factor of 10^8; in parentheses, we also provide the condition number estimate of T, with the mantissa rounded to the nearest integer. The initial guess was always equal to zero. If the convergence criterion was not reached in 100 iterations, we place a dash. Experiments which were not performed due to hardware limitations are marked with 'N/A'. For comparison, we also include results when the
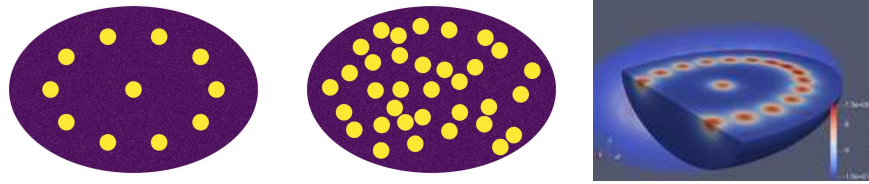
Fig. 1: Types of domains and subdomains. Left: elliptic shaped Ω with regularly placed circular $N = 11$ organelles. Center: elliptic shaped Ω with randomly placed nonoverlapping circular $N = 33$ organelles. Right: 3D ellipsoid with regularly placed organelles (visualized is a cross–section of the domain; colors reflect the value of the solution).

$\downarrow r \rightarrow p$	1	2	3
16	$4.4 \cdot 10^2$	$1.7 \cdot 10^3$	$3.7 \cdot 10^3$
32	$1.7 \cdot 10^3$	$6.5 \cdot 10^3$	$1.4 \cdot 10^4$
64	$6.2 \cdot 10^3$	$2.5 \cdot 10^4$	$5.5 \cdot 10^4$
128	$2.5 \cdot 10^4$	$9.7 \cdot 10^4$	$2.2 \cdot 10^5$

$\downarrow r \rightarrow p$	1	2	3
16	$1.3 \cdot 10^4$	$9.6 \cdot 10^4$	$3.2 \cdot 10^5$
24	$6.1 \cdot 10^4$	$4.7 \cdot 10^5$	N/A
32	$9.6 \cdot 10^4$	$7.4 \cdot 10^5$	N/A

Table 1: Approximate total number of degrees of freedom for various values of mesh resolution parameter r and polynomial degree p. Left: 2D case; right: 3D case.

problem was solved with the PCG, where the BoomerAMG was used to precondition the whole discrete system resulting from Problem 2.

While varying other parameters, if not specified otherwise, we assume default values $\varrho = K = 1$, $p = 2$, $N = 22$ and $r = 128$ in 2D case or $r = 32$ in 3D case. In Tables 2–3 we investigate the dependence of the convergence rate on r, p, ϱ, K for both moderate and very large value of G. It turns out that the performance of T is essentially uniform across the range (with some small degradation for certain extreme values of ϱ or K) regardless of G, while the AMG suffers for most combinations of parameters when G is large. Tables 6–7 confirm analogous behavior in 3D.

In Table 4 we repeat the first experiment with irregularly scattered organelles (cf. the middle picture in Figure 1) with no significant differences. From Table 5 it follows T performs well, independently of the number of inclusions, again, with some increase of the number of iterations for large ϱ.

Finally, in Table 8 we provide more detailed insight into the convergence rate of T for G in the range $10^0 \ldots 10^{12}$, while keeping other parameters fixed. It turns out that the number of iterations of T stays essentially constant.

4 Conclusions

Numerical experiments indicate the preconditioner under consideration performs well in a broad range of problem parameters. The main advantage of the proposed preconditioner over the AMG preconditioner applied directly to the discrete prob-

$\downarrow r \rightarrow p$	1	2	3	1	2	3
16	$10\,(2 \cdot 10^0)$	$10\,(2 \cdot 10^0)$	$10\,(2 \cdot 10^0)$	$6\,(1 \cdot 10^0)$	$6\,(1 \cdot 10^0)$	$7\,(1 \cdot 10^0)$
32	$10\,(2 \cdot 10^0)$	$10\,(2 \cdot 10^0)$	$10\,(2 \cdot 10^0)$	$6\,(1 \cdot 10^0)$	$6\,(1 \cdot 10^0)$	$7\,(1 \cdot 10^0)$
64	$10\,(2 \cdot 10^0)$	$10\,(2 \cdot 10^0)$	$10\,(2 \cdot 10^0)$	$6\,(1 \cdot 10^0)$	$6\,(1 \cdot 10^0)$	$7\,(1 \cdot 10^0)$
128	$10\,(2 \cdot 10^0)$	$10\,(2 \cdot 10^0)$	$11\,(2 \cdot 10^0)$	$6\,(1 \cdot 10^0)$	$7\,(1 \cdot 10^0)$	$7\,(1 \cdot 10^0)$
16	$7\,(2 \cdot 10^0)$	$9\,(2 \cdot 10^0)$	$11\,(3 \cdot 10^0)$	$46\,(3 \cdot 10^5)$	$96\,(3 \cdot 10^5)$	$-$
32	$9\,(2 \cdot 10^0)$	$9\,(2 \cdot 10^0)$	$11\,(2 \cdot 10^0)$	$69\,(3 \cdot 10^5)$	$-$	$-$
64	$9\,(2 \cdot 10^0)$	$10\,(2 \cdot 10^0)$	$11\,(2 \cdot 10^0)$	$92\,(3 \cdot 10^5)$	$-$	$-$
128	$9\,(2 \cdot 10^0)$	$10\,(2 \cdot 10^0)$	$11\,(3 \cdot 10^0)$	$-$	$-$	$-$

Table 2: Iteration count (the condition number estimate in parentheses) for varying mesh resolution r and polynomial degree p: T (left) vs. AMG preconditioner (right). Top: $G = 10^0$; bottom: $G = 10^6$. 2D case, regularly placed $N = 22$ subdomains. $\varrho = K = 1$.

$\downarrow \varrho \rightarrow K$	10^{-6}	10^0	10^6	10^{-6}	10^0	10^6
10^{-6}	$10\,(2 \cdot 10^0)$	$10\,(2 \cdot 10^0)$	$10\,(2 \cdot 10^0)$	$13\,(3 \cdot 10^0)$	$13\,(3 \cdot 10^0)$	$7\,(1 \cdot 10^0)$
10^0	$12\,(3 \cdot 10^0)$	$10\,(2 \cdot 10^0)$	$10\,(2 \cdot 10^0)$	$9\,(2 \cdot 10^0)$	$7\,(1 \cdot 10^0)$	$7\,(1 \cdot 10^0)$
10^6	$15\,(4 \cdot 10^0)$	$13\,(3 \cdot 10^0)$	$11\,(2 \cdot 10^0)$	$11\,(2 \cdot 10^0)$	$9\,(1 \cdot 10^0)$	$7\,(1 \cdot 10^0)$
10^{-6}	$11\,(2 \cdot 10^0)$	$12\,(3 \cdot 10^0)$	$11\,(2 \cdot 10^0)$	$-$	$-$	$40\,(4 \cdot 10^1)$
10^0	$10\,(2 \cdot 10^0)$	$10\,(2 \cdot 10^0)$	$11\,(2 \cdot 10^0)$	$-$	$-$	$40\,(4 \cdot 10^1)$
10^6	$14\,(3 \cdot 10^0)$	$13\,(3 \cdot 10^0)$	$10\,(2 \cdot 10^0)$	$52\,(1 \cdot 10^6)$	$44\,(7 \cdot 10^5)$	$13\,(3 \cdot 10^0)$

Table 3: Iteration count (the condition number estimate in parentheses) for varying contrast ratios ϱ and K for T (left) vs. AMG preconditioner (right). Top: $G = 10^0$; bottom: $G = 10^6$. 2D case, regularly placed $N = 22$ subdomains. $r = 128$, $p = 2$.

$\downarrow r \rightarrow p$	1	2	3	1	2	3
16	$9\,(2 \cdot 10^0)$	$9\,(2 \cdot 10^0)$	$10\,(2 \cdot 10^0)$	$6\,(1 \cdot 10^0)$	$6\,(1 \cdot 10^0)$	$7\,(1 \cdot 10^0)$
32	$10\,(2 \cdot 10^0)$	$10\,(2 \cdot 10^0)$	$10\,(2 \cdot 10^0)$	$6\,(1 \cdot 10^0)$	$6\,(1 \cdot 10^0)$	$7\,(1 \cdot 10^0)$
64	$10\,(2 \cdot 10^0)$	$10\,(2 \cdot 10^0)$	$10\,(2 \cdot 10^0)$	$6\,(1 \cdot 10^0)$	$6\,(1 \cdot 10^0)$	$7\,(1 \cdot 10^0)$
128	$10\,(2 \cdot 10^0)$	$10\,(2 \cdot 10^0)$	$10\,(2 \cdot 10^0)$	$6\,(1 \cdot 10^0)$	$7\,(1 \cdot 10^0)$	$8\,(1 \cdot 10^0)$
16	$7\,(2 \cdot 10^0)$	$9\,(2 \cdot 10^0)$	$10\,(2 \cdot 10^0)$	$32\,(2 \cdot 10^5)$	$64\,(3 \cdot 10^5)$	$93\,(3 \cdot 10^5)$
32	$8\,(2 \cdot 10^0)$	$9\,(2 \cdot 10^0)$	$11\,(2 \cdot 10^0)$	$68\,(3 \cdot 10^5)$	$-$	$-$
64	$9\,(2 \cdot 10^0)$	$10\,(2 \cdot 10^0)$	$11\,(2 \cdot 10^0)$	$85\,(3 \cdot 10^5)$	$-$	$-$
128	$10\,(2 \cdot 10^0)$	$10\,(2 \cdot 10^0)$	$12\,(3 \cdot 10^0)$	$-$	$-$	$-$

Table 4: Iteration count (the condition number estimate in parentheses) for varying mesh resolution r and polynomial degree p: T (left) vs. AMG preconditioner (right). Top: $G = 10^0$ bottom: $G = 10^6$. 2D case, irregularly placed $N = 19$ subdomains. $\varrho = K = 1$.

lem is the robustness of the former with respect to the permeability parameter G. Theoretical analysis of the preconditioner will be presented elsewhere.

$\to N$	19	35	51	19	35	51
$\downarrow \varrho$						
10^{-6}	$10\,(2 \cdot 10^0)$	$10\,(2 \cdot 10^0)$	$11\,(2 \cdot 10^0)$	$12\,(3 \cdot 10^0)$	$13\,(3 \cdot 10^0)$	$16\,(4 \cdot 10^0)$
10^{0}	$10\,(2 \cdot 10^0)$	$10\,(2 \cdot 10^0)$	$10\,(2 \cdot 10^0)$	$7\,(1 \cdot 10^0)$	$7\,(1 \cdot 10^0)$	$7\,(1 \cdot 10^0)$
10^{6}	$12\,(2 \cdot 10^0)$	$13\,(3 \cdot 10^0)$	$14\,(3 \cdot 10^0)$	$8\,(1 \cdot 10^0)$	$9\,(1 \cdot 10^0)$	$10\,(1 \cdot 10^0)$
10^{-6}	$11\,(2 \cdot 10^0)$	$11\,(2 \cdot 10^0)$	$11\,(2 \cdot 10^0)$	–	–	–
10^{0}	$10\,(2 \cdot 10^0)$	$10\,(2 \cdot 10^0)$	$10\,(2 \cdot 10^0)$	–	–	–
10^{6}	$13\,(3 \cdot 10^0)$	$13\,(3 \cdot 10^0)$	$13\,(3 \cdot 10^0)$	$44\,(7 \cdot 10^5)$	$61\,(7 \cdot 10^5)$	$69\,(9 \cdot 10^5)$

Table 5: Iteration count (the condition number estimate in parentheses) for varying contrast ratios ϱ and number of subdomains N: T (left) vs. AMG preconditioner (right). Top: $G = 10^0$ bottom: $G = 10^6$. 2D case, irregularly placed subdomains. $r = 128$, $p = 2$, $K = 1$.

$\downarrow r \to p$	1	2	3	1	2	3
24	$10\,(2 \cdot 10^0)$	$10\,(2 \cdot 10^0)$	$11\,(3 \cdot 10^0)$	$5\,(1 \cdot 10^0)$	$7\,(2 \cdot 10^0)$	$9\,(2 \cdot 10^0)$
32	$9\,(2 \cdot 10^0)$	$9\,(2 \cdot 10^0)$	N/A	$5\,(1 \cdot 10^0)$	$6\,(1 \cdot 10^0)$	N/A
48	$9\,(2 \cdot 10^0)$	$10\,(2 \cdot 10^0)$	N/A	$5\,(1 \cdot 10^0)$	$6\,(1 \cdot 10^0)$	N/A
32	$8\,(2 \cdot 10^0)$	$10\,(2 \cdot 10^0)$	$11\,(3 \cdot 10^0)$	$86\,(1 \cdot 10^5)$	–	–
64	$7\,(2 \cdot 10^0)$	$9\,(2 \cdot 10^0)$	N/A	$83\,(1 \cdot 10^5)$	–	N/A
128	$8\,(2 \cdot 10^0)$	$9\,(2 \cdot 10^0)$	N/A	$92\,(1 \cdot 10^5)$	–	N/A

Table 6: Iteration count (the condition number estimate in parentheses) for varying mesh resolution r and polynomial degree p: T (left) vs. AMG preconditioner (right). Top: $G = 10^0$ bottom: $G = 10^6$. 3D case. $\varrho = K = 1$, $N = 22$.

$\downarrow \varrho \to K$	10^{-6}	10^{0}	10^{6}	10^{-6}	10^{0}	10^{6}
10^{-6}	$9\,(2 \cdot 10^0)$	$11\,(2 \cdot 10^0)$	$12\,(2 \cdot 10^0)$	$9\,(2 \cdot 10^0)$	$10\,(2 \cdot 10^0)$	$12\,(2 \cdot 10^0)$
10^{0}	$10\,(2 \cdot 10^0)$	$10\,(2 \cdot 10^0)$	$12\,(2 \cdot 10^0)$	$7\,(1 \cdot 10^0)$	$6\,(1 \cdot 10^0)$	$12\,(2 \cdot 10^0)$
10^{6}	$12\,(3 \cdot 10^0)$	$11\,(2 \cdot 10^0)$	$9\,(2 \cdot 10^0)$	$9\,(1 \cdot 10^0)$	$8\,(1 \cdot 10^0)$	$6\,(1 \cdot 10^0)$
10^{-6}	$9\,(2 \cdot 10^0)$	$11\,(2 \cdot 10^0)$	$15\,(3 \cdot 10^0)$	–	–	$42\,(3 \cdot 10^1)$
10^{0}	$9\,(2 \cdot 10^0)$	$9\,(2 \cdot 10^0)$	$15\,(3 \cdot 10^0)$	–	–	$42\,(3 \cdot 10^1)$
10^{6}	$12\,(3 \cdot 10^0)$	$12\,(3 \cdot 10^0)$	$10\,(2 \cdot 10^0)$	$34\,(6 \cdot 10^5)$	$33\,(5 \cdot 10^5)$	$14\,(4 \cdot 10^0)$

Table 7: Iteration count (the condition number estimate in parentheses) for varying contrast ratios ϱ and K: T (left) vs. AMG preconditioner (right). Top: $G = 10^0$; bottom: $G = 10^6$. 3D case, $r = 32$, $p = 2$, $N = 22$.

References

1. M. S. Alnæs, J. Blechta, J. Hake, A. Johansson, B. Kehlet, A. Logg, C. Richardson, J. Ring, M. E. Rognes, and G. N. Wells. The FEniCS Project Version 1.5. *Archive of Numerical Software*, 3(100), 2015.

2. P. F. Antonietti and P. Houston. A class of domain decomposition preconditioners for hp-discontinuous Galerkin finite element methods. *J. Sci. Comput.*, 46(1):124–149, 2011.

3. P. F. Antonietti, P. Houston, G. Pennesi, and E. Süli. An agglomeration-based massively parallel non-overlapping additive Schwarz preconditioner for high-order discontinuous Galerkin methods on polytopic grids. *Math. Comp.*, 89(325):2047–2083, 2020.

G	10^0	10^2	10^4	10^6	10^8	10^{10}	10^{12}
T	$10\,(2\cdot10^0)$	$10\,(2\cdot10^0)$	$10\,(2\cdot10^0)$	$10\,(2\cdot10^0)$	$10\,(2\cdot10^0)$	$10\,(2\cdot10^0)$	$10\,(2\cdot10^0)$
AMG	$7\,(1\cdot10^0)$	$39\,(3\cdot10^1)$	–	–	–	–	–
T	$10\,(2\cdot10^0)$	$10\,(2\cdot10^0)$	$9\,(2\cdot10^0)$	$9\,(2\cdot10^0)$	$9\,(2\cdot10^0)$	$9\,(2\cdot10^0)$	$9\,(2\cdot10^0)$
AMG	$6\,(1\cdot10^0)$	$31\,(2\cdot10^1)$	–	–	–	–	–

Table 8: Iteration count (the condition number estimate in parentheses) for varying permeability coefficient G. Regularly placed $N = 18$ subdomains. Top: 2D case ($r = 128$), bottom: 3D case ($r = 32$). $\varrho = K = 1$, $p = 2$.

4. P. F. Antonietti, P. Houston, and I. Smears. A note on optimal spectral bounds for nonoverlapping domain decomposition preconditioners for hp-version Discontinuous Galerkin method. *Int. J. Numer. Anal. Model.*, 13(4):513–524, 2016.

5. P. F. Antonietti, M. Sarti, M. Verani, and L. T. Zikatanov. A uniform additive Schwarz preconditioner for high-order discontinuous Galerkin approximations of elliptic problems. *J. Sci. Comput.*, 70(2):608–630, 2017.

6. S. Balay, S. Abhyankar, M. F. Adams, J. Brown, P. Brune, K. Buschelman, L. Dalcin, V. Eijkhout, W. D. Gropp, D. Kaushik, M. G. Knepley, D. A. May, L. C. McInnes, K. Rupp, P. Sanan, B. F. Smith, S. Zampini, H. Zhang, and H. Zhang. PETSc users manual. Technical Report ANL-95/11 - Revision 3.8, Argonne National Laboratory, 1995–.

7. M. A. J. Chaplain, C. Giverso, T. Lorenzi, and L. Preziosi. Derivation and application of effective interface conditions for continuum mechanical models of cell invasion through thin membranes. *SIAM J. Appl. Math.*, 79:2011–2031, 2019.

8. M. Dryja. On discontinuous Galerkin methods for elliptic problems with discontinuous coefficients. *Comput. Methods Appl. Math.*, 3(1):76–85 (electronic), 2003.

9. M. Dryja and P. Krzyżanowski. A massively parallel nonoverlapping additive Schwarz method for discontinuous Galerkin discretization of elliptic problems. *Num. Math.*, 132(2):347–367, 2015.

10. M. Dryja and M. Sarkis. Additive average Schwarz methods for discretization of elliptic problems with highly discontinuous coefficients. *Comput. Methods Appl. Math.*, 10(2):164–176, 2010.

11. R. D. Falgout, J. E. Jones, and U. M. Yang. The design and implementation of hypre, a library of parallel high performance preconditioners. In *Numerical solution of Partial Differential Equations on Parallel Computers, Lect. Notes Comput. Sci. Eng*, pages 267–294. Springer-Verlag, 2006.

12. P. Krzyżanowski. On a nonoverlapping additive Schwarz method for h-p discontinuous Galerkin discretization of elliptic problems. *Num. Meth. PDEs*, 32(6):1572–1590, 2016.

13. P. Krzyżanowski. Simple preconditioner for a thin membrane diffusion problem. In R. Wyrzykowski, E. Deelman, J. Dongarra, and K. Karczewski, editors, *Parallel Processing and Applied Mathematics*, volume 12044 LNCS, pages 267–276, Cham, 2020. Springer International Publishing.

14. M. Sturrock, A. J. Terry, D. P. Xirodimas, A. M. Thompson, and M. A. J. Chaplain. Influence of the nuclear membrane, active transport, and cell shape on the hes1 and p53–mdm2 pathways: Insights from spatio-temporal modelling. *Bulletin of Mathematical Biology*, 74(7):1531–1579, Jul 2012.

15. A. Toselli and O. Widlund. *Domain decomposition methods—algorithms and theory*, volume 34 of *Springer Series in Computational Mathematics*. Springer-Verlag, Berlin, 2005.

16. J. Xu and L. Zikatanov. Algebraic multigrid methods. *Acta Numerica*, 26:591–721, 2017.